8-1-1992

Formation of a Square-Planar Co(I) B12 Intermediate. Implications for Enzyme Catalysis

Mark R. Chance
Case Western Reserve University, mark.chance@case.edu

Author(s) ORCID Identifier:

Mark R. Chance

Recommended Citation
M.D. Wirt, I. Sagi, M.R. Chance. Formation of a square-planar Co(I) B12 intermediate. Implications for enzyme catalysis. Biophysical Journal, Volume 63, Issue 2, 1992, Pages 412-417, https://doi.org/10.1016/S0006-3495(92)81605-3.

Formation of a square-planar Co(I) B_{12} intermediate

Implications for enzyme catalysis

Michael D. Wirt, Irit Sagi, and Mark R. Chance
Department of Chemistry, Georgetown University, Washington, DC 20057 USA

ABSTRACT X-ray edge and extended x-ray absorption fine structure (EXAFS) techniques provide powerful tools for analysis of local molecular structure of complexes in solution. We present EXAFS results for Co(I) B_{12} that demonstrate a four-coordinate (distorted) square-planar configuration. Comparison of EXAFS solutions for Co(I) and Co(II) B_{12} (collected previously; Sagi et al. 1990. *J. Am. Chem. Soc.* 112:8639–8644) suggest that modulation of the Co—N bond to the axial 5,6-dimethylbenzimidazole (DMB), in the absence of changes in Co—N (equatorial) bond distances, may be a key mechanism in promoting homolytic versus heterolytic cleavage. As Co—C bond homolysis occurs, the Co—N (DMB) bond becomes stronger. However, for heterolytic cleavage to occur, earlier electrochemical studies (D. Lexa and J. M. Saveant. 1976. *J. Am. Chem. Soc.* 98:2652–2658) and recent studies of methylcobalamin-dependent *Clostridium thermoaceticum* (Ragsdale et al. 1987. *J. Biol. Chem.* 262:14289–14297) suggest that removal of the DMB ligand (before Co—C bond cleavage) favors formation of the four-coordinate square-planar Co(I) species while inhibiting formation of the five-coordinate Co(II) B_{12} complex. This paper presents the first direct evidence that formation of the Co(I) B_{12} intermediate must involve breaking of the Co—N (DMB) bond.

INTRODUCTION

5′-Deoxyadenosylcobalamin (AdoCbl) (Fig. 1) functions as an essential cofactor for enzyme reactions involving 1,2 exchange of a hydrogen atom and a second functional group, such as $-NH_2$ in ethanolamine ammonia lyase or —OH in diol dehydrase (1). The mechanism of Co—C bond cleavage for these reactions is well established as homolytic, forming a primary alkyl radical and the Co(II) B_{12} intermediate (2). In addition, valuable information regarding the mechanism of Co(II) B_{12} formation has been derived from bond dissociation energy studies of Halpern and others (2–5). In these studies, the primary role of AdoCbl is identified to be that of a free radical precursor. Although nonhomolytic cleavage mechanisms for B_{12}-dependent enzymes have been proposed for years, only recently has substantial work been completed on two methylcobalamin (MeCbl)-dependent enzymes that are believed to proceed through a Co(I) B_{12} intermediate (6–8).

We present structural data, derived from extended x-ray absorption fine structure (EXAFS) and x-ray edge spectroscopy, that definitively demonstrate a four-coordinate (distorted) square-planar configuration for Co(I) B_{12}. For both homolytic and heterolytic reactions, knowledge of the mechanism of Co—C cleavage and the structure of the intermediates is critical to understanding how cleavage is accelerated by enzymes. A key question concerns the structural features of alkyl cobalamins that are regulated by enzymes to favor homolysis versus heterolysis. Modulation of the Co—5,6-dimethylbenzimidazole (DMB) bond may be a key factor in the mechanism of Co—C bond cleavage and the formation of four-coordinate Co(I) B_{12} intermediates.

Address correspondence to Mark R. Chance at the Department of Physiology and Biophysics, Albert Einstein College of Medicine, Bronx, New York 10461.

MATERIALS AND METHODS

Materials

Cyanocobalamin and sodium borohydride were obtained from Sigma Chemical Co. (St. Louis, MO). Aluminum oxide and 5,10,15,20-tetraphenyl-21H,23H-porphine Co(II) (CoTPP) were purchased from Aldrich Chemical Co. (Milwaukee, WI). Glycerol was obtained from Fisher Scientific Co. (Pittsburgh, PA). All were used without further purification. Cyanocobalamin purity was verified by optical spectroscopy. We tested the glycerol, borohydride, and aluminum oxide in solution and solid form for the presence of cobalt by x-ray absorption before sample preparation. No detectable edge jump was observed for the test samples; therefore, the cobalt concentration in these samples was <0.5% of that in the experimental samples and could be ignored.

Sample preparation

Co(I) B_{12} was prepared by reduction of 1.5 ml of 12 mM cyanocobalamin with 0.7 ml of 0.8 M $NaBH_4$ under argon as described by Dolphin (9). The cyanocobalamin and $NaBH_4$ solutions were degassed with argon for 30 min before reduction. Co(II) B_{12} was formed from the addition of 0.5 ml of $NaBH_4$ to 1.5 ml of 12 mM cyanocobalamin. Co(I) B_{12} was prepared via the Co(II) intermediate, by adding an additional 0.2 ml of 0.8 M $NaBH_4$ solution, under argon, to the yellow-brown solution of Co(II) B_{12} with constant stirring. The Co(II) B_{12} solution immediately turned to the dark blue-green Co(I) B_{12} species (9). All samples were prepared as solutions in 35% glycerol to reduce sample cracking on freezing, with the exception of CoTPP, which was a solid. All samples were placed in 25 × 2.5 × 2-mm-deep lucite sample holders covered with mylar tape (approximate volume 200 μl). To minimize fluorescence saturation effects, solid samples were diluted with aluminum oxide and ground to a fine powder in a mortar and pestle. The mixed powder was packed in a lucite sample holder. All solid samples were diluted 1:10 by weight in aluminum oxide. The liquid samples were anaerobically transferred into the sample holders under argon and immediately submerged in liquid nitrogen.

0006-3495/92/08/412/06 $2.00

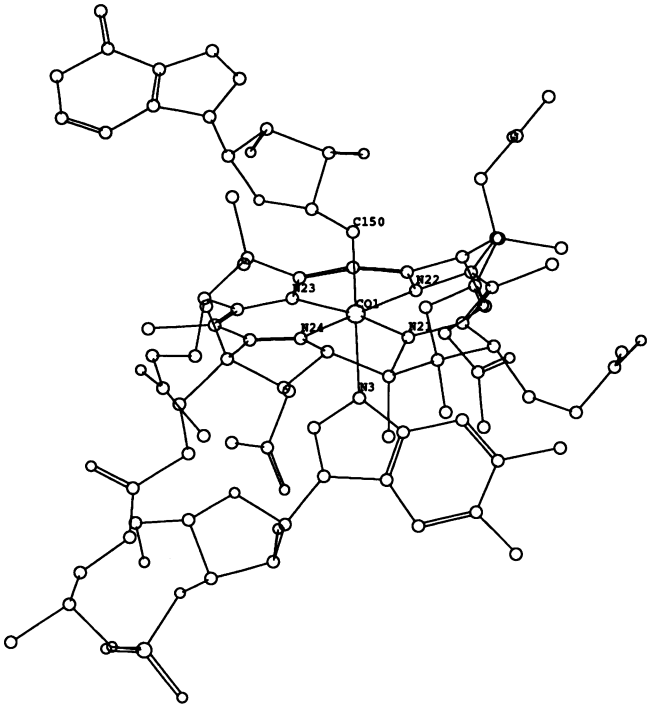

FIGURE 1 Structure of AdoCbl.

X-ray absorption data were collected on several Co(I) B_{12} samples that were characterized before and after data collection by optical spectroscopy. Optical characterization was accomplished by transferring concentrated samples under argon to stoppered cuvettes containing deionized water that were previously degassed for 15 min. Immediately after sample transfer, the cuvette was sealed, and an optical spectrum was taken. The Co(I) B_{12} spectra were consistent with earlier absorption spectra of Beaven and Johnson (10). Percent conversion from cyanocobalamin to Co(I) B_{12} was calculated at 93 ± 2%. The presence of cyanocobalamin in the Co(I) B_{12} samples was measured by observing the remaining height of the 361-nm cyanocobalamin parent peak. This was accomplished by fitting a cubic polynomial to the baseline of the pure cyanocobalamin and Co(I) B_{12} spectra to normalize the peak heights. The absolute peak height was determined, allowing calculation of the percent cyanocobalamin remaining in the Co(II) species (5% by this method). In addition, the percent unconverted Co(II) remaining in the Co(I) sample was calculated in a similar fashion by using the 312-nm peak of the Co(II) B_{12} as an indicator (2% by this method). A second method for analyzing the percent conversion to the Co(I) B_{12} species involved fitting the region from 280 to 390 nm by a sum of Gaussian bands. Analysis of three peaks in the Co(I) B_{12} spectrum, at 386 nm [from Co(I) B_{12}], at 361 nm (from cyanocobalamin), and at 312 nm [from Co(II) B_{12}], gave a ratio of Co(I) to cyanocobalamin and Co(II) of 19:1 or a total of 5% Co(II) and cyanocobalamin remaining. Great care was taken to stabilize the reactive Co(I) species by freeze trapping and irradiating the sample at ≤150 K. Additionally, shifts in the cobalt absorption threshold (main peak of the first derivative of the x-ray absorption spectrum) are characteristic of the effective charge on the cobalt ion. Edge shifts to lower energy for the chemical reduction of Co(III) to Co(II) to Co(I) B_{12} follow a linear relationship between the absorption threshold position and the effective charge of the metal (11). Thus, the sample integrity is verified by examination of the edge position of each scan as well as the optical spectrum after data collection.

Data collection

X-ray fluorescence data were collected at the National Synchrotron Light Source, Brookhaven National Laboratory (Upton, New York) on beam line X-9A, using a double flat Si(111) crystal monochromator with fixed exit geometry. All experiments were carried out at 140–150 K, and sample temperature was maintained by flowing cooled nitrogen gas through a low-temperature cryostat as described previously (12). X-ray edge data having 3 eV resolution were recorded by counting at a specific energy for 2 s and incrementing the energy by 0.5 eV from 20 eV below the cobalt edge to 50 eV above the edge. EXAFS data, also having 3 eV resolution, were recorded by counting at a specific energy for 4 s and incrementing the energy by 10 eV from 120 eV below the cobalt edge to 20 eV below the edge, then in 1.0 eV steps to 15 eV above the edge, and finally in 3.0 eV steps from that point to 600 eV above the edge. A total of 15 scans were collected from three different samples. Photon flux was 3.75×10^{11} photons/s at 100-ma beam current (13); both EXAFS and x-ray edge data were generally taken in the range of 90–180 ma. Cyanocobalamin was used as a standard to account for any shifts in the monochromator. K-α cobalt fluorescence was detected with a zinc sulfide-coated photomultiplier tube (14), and incident photon scattering was rejected by an iron oxide filter. Output signals were amplified with a Keithley amplifier, converted to frequency, and counted in a scaler interfaced to a PDP 11/23+ Digital computer via CAMAC. For reference signals, mylar tape was mounted at a 45° angle to the x-ray beam to scatter photons counted by a similar photomultiplier tube positioned perpendicular to the x-ray beam. This method provided excellent linearity between the sample and the reference detectors.

Data analysis and errors

EXAFS background removal, k^3-weighting, Fourier filtering, and nonlinear least-squares fitting followed standard procedures (15–17). Raw, unsmoothed, undeglitched data were used for the analysis. Background subtracted data were Fourier transformed with use of cosine-squared tapered windows as described previously (15). The taper ends had centers of 1.5 and 10.2 $Å^{-1}$ in k-space. The Fourier filter back-transform window taper centers were set to 0.8 and 1.9 $Å^{-1}$. At $k_1 - Dk_1/2$ and $k_2 + Dk_2/2$, the window function tailed to zero, and at $k_1 + Dk_1/2$ and $k_2 - Dk_2/2$, the window function was completely square and left unchanged (where D is an arbitrary value that simply selects the degree of taper). The back-transform (r window function) was the same type as the k window function. The taper functions were set at $Dk_1 = Dk_2 = 3.0$ $Å^{-1}$. The Fourier filter window taper functions were set to $Dr_1 = Dr_2 = 0.2$ Å. All data were fit from 3.5 to 10.0 $Å^{-1}$ in k-space. The EXAFS solution was obtained by fitting the Co(I) B_{12} data to CoTPP, which has a well-known crystal structure (18), by means of the University of Washington EXAFS package on the Georgetown 8700 VAX computer (15). The CoTPP model compound data were treated in the same manner as the Co(I) B_{12} samples.

Errors in the EXAFS analysis were estimated by three methods. First, partial sums of the total number of scans for a single sample were independently fit. The differences in fit distances provide an estimate of random noise. Second, independently prepared samples were analyzed separately to measure errors due to sample preparations, radiation damage, and other related nonrandom fluctuations. Third, the method of mapping out the minimum solution by examination of χ^2 was applied. This method was conducted as follows: the error bar associated with a particular parameter in the fit was obtained by fixing that parameter at specific values, while least-squares refining the others, until χ^2 was double that of the minimum solution (19). These error estimates gave similar results of ±0.01–0.02 Å for distances.

RESULTS AND DISCUSSION

Fig. 2 shows the undeglitched, unsmoothed, wave vector cubed, background subtracted data for the reduced Co(I) B_{12} species. The Fourier transform of the undeglitched, unsmoothed data in Fig. 2 is presented in Fig. 3. A one-atom type fit with free parameters of distance, coordina-

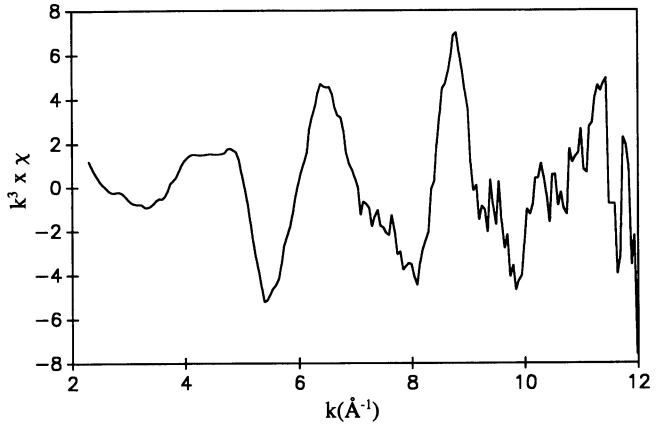

FIGURE 2 Undeglitched unsmoothed wave vector-cubed background subtracted data of Co(I) B_{12}. Data were Fourier transformed from 1.5 to 10.2 Å^{-1} in k-space with cosine-squared tapered windows as described in text.

TABLE 1 Nonlinear least-squares fitting solutions for Co(I) B_{12} EXAFS spectra

Solution	Model	r	N	ΔE_0	$\Delta\sigma^2$	χ^2
		Å		eV	Å^{-2}	
A	Co—N	1.88	3.0	−1	-2×10^{-3}	1.5
B	Co—N	1.88	3.5	−2	-6×10^{-4}	0.8
C	Co—N	1.88	4.0	−2	5×10^{-4}	1.7
D	Co—N	1.89	4.5	−3	2×10^{-3}	3.3
E	Co—N	1.89	5.0	−4	3×10^{-3}	5.8

Simulated solutions A–E represent fitting results at various values of fixed coordination number. All solutions result from fixing N, letting r and σ^2 float, and stepping E_0 from −8 to +8 eV to minimize χ^2. EXAFS solutions for Co(I) B_{12} are obtained from Fourier filtered data. The back-transformed data are fit to CoTPP (4 nitrogens at 1.949 Å average distance) by a nonlinear least-squares fitting procedure. Parameters: r, distance in Å; N, coordination number; ΔE_0, energy shift relative to model compound; $\Delta\sigma^2$, Debye-Waller shift relative to model compound; χ^2, sum of residuals squared.

tion number, Debye-Waller factor shift, and edge energy shift (the latter two with respect to the model compound) gives a solution of 1.88 ± 0.02 Å, 3.5 ± 0.6 ligands, $\Delta\sigma^2 = -6 \times 10^{-4} \pm 0.0001$ Å^{-2}, $\Delta E_0 = -2.0$ eV, χ^2 (sum of the residuals squared) = 0.8, respectively. The back-transformed data of Co(I) B_{12} compared with the one-atom fit simulated solution B (Table 1) (reported above) are presented in Fig. 4. The agreement between the Co(I) B_{12} data and the simulation is excellent.

To examine the dependence of the EXAFS solution on coordination number (N), a series of fits were carried out with N fixed at various values to judge the effect on χ^2 and Debye-Waller factors (Table 1). When N is held fixed at 3.0, χ^2 doubles, and it also nearly doubles at $N \geq 4.0$. This provides the error range of the coordination number for this data set (19). When N is fixed at 5.0, the χ^2 is over seven times that of the minimum solution and nearly four times that of $N = 4.0$. These comparisons provide good evidence that coordination numbers of three or four are supported by the data. However, a coordination number of three is not chemically reasonable for the cobalt-corrin system. All of the E_0 and Debye-Waller factor shifts in Table 1 are chemically reasonable (16, 20, 21). Two different two-atom type fits were attempted in addition to the one-atom fits: a (3 Co—N):(1 Co—N) and a (2 Co—N):(2 Co—N) fit. Although these fits gave χ^2 values superior to those of the one-atom fit, this is to be expected because of the increased number of free parameters. Of greater importance is that these minima either had chemically unreasonable Debye-Waller factors or had distance solutions whose differences were less than the resolution of the data. Thus, a one-atom fit is sufficient to simulate the data.

Integration of preedge transitions of x-ray absorption spectra and comparison of these intensities to model compounds provide a means for predicting geometric conformations (11, 22, 23). The edge spectrum of Co(I) B_{12} contains a moderate intensity 1s-4p + shake-down (transfer of charge from ligand to metal, SD) peak and no 1s-3d transition (Fig. 5). The absence of a 1s-3d tran-

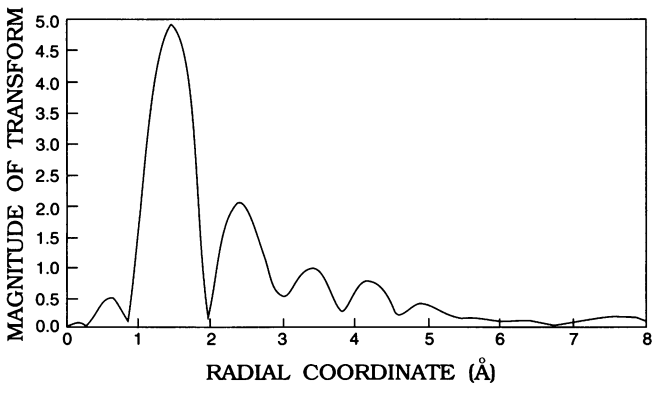

FIGURE 3 Fourier transform of undeglitched unsmoothed background subtracted data of data seen in Fig. 2.

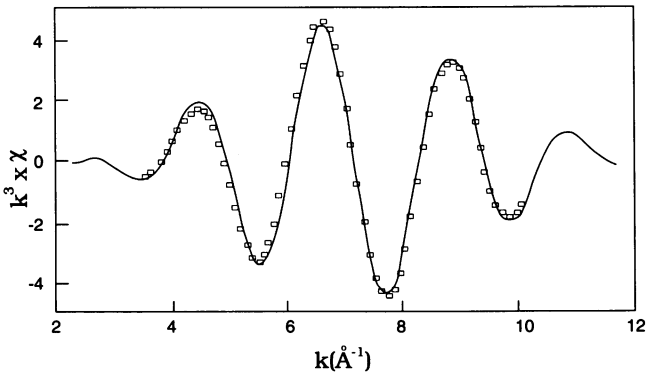

FIGURE 4 Back-transformed undeglitched unsmoothed data of Co(I) B_{12} (*solid lines*) compared with the 1-atom fit simulated solution B (*squares*); $\chi^2 = 0.8$. Data are fit from 3.5 to 10.0 Å^{-1} in k-space.

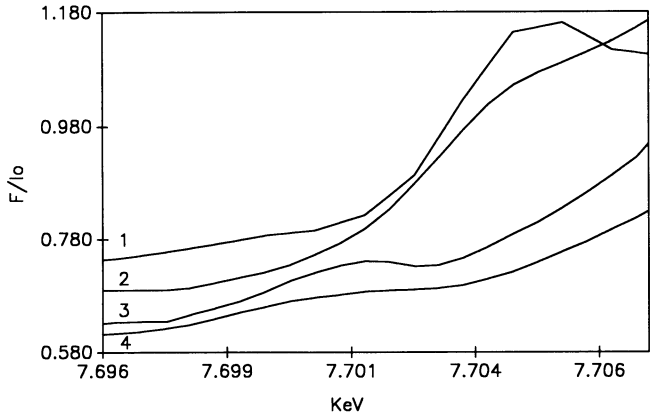

FIGURE 5 Comparison of x-ray fluorescence preedge data of transitions observed in cobalt model and cobalamin compounds: (*1*) CoTPP, 1s-4p + shake-down (4-coordinate; not to scale compared with other spectra); (*2*) Co(I) B_{12}, 1s-4p + shake-down (4-coordinate); (*3*) Co(II) B_{12}, 1s-3d (5-coordinate); and (*4*) cyanocobalamin, 1s-3d (6-coordinate).

sition indicates that neither coordination number five nor tetrahedral geometries are present (22, 23). The presence of the 1s-4p + SD peak confirms the square-planar assignment. Extensive studies of square-planar copper chlorides (24, 25) and nickel tetracyanide complexes (26) have been used in an attempt to establish a theoretical basis for the 1s-4p + SD transition. Kosugi et al. (25), using polarized synchrotron radiation on single crystals of $(creatinium)_2CuCl_4$, established that 1s-4p + SD transitions have a strong z dependency (where the z axis is normal to the molecular plane) (25). The relationship between the shake-down process and square planar geometry may lie in the interaction of the empty $4p_z$ metal orbital with ligand orbitals from which charge transfer to the metal can occur. CoTPP, a nearly perfect square-planar complex (18), shows a much larger intensity for the 1s-4p + SD peak than Co(I) B_{12} (Fig. 5). Co(I) B_{12} will deviate from a pure planar geometry due to the fusion of corrin tetrapyrrole rings A and D (Fig. 1). This would tend to reduce the 1s-4p + SD transition intensity if it decreases the interaction between the ligands and the $4p_z$ orbital. A square-planar configuration for Co(I) B_{12} has been previously considered based on electronic absorption (10, 27) and electrochemical studies of Lexa and Saveant (28, 29). Our x-ray edge and EXAFS data provide direct evidence for the four-coordinate (distorted) square-planar conformation predicted by these earlier studies.

Susceptibility of the Co—C bond to homolytic cleavage is modulated by steric repulsion between the alkyl group and the corrin ring (2), as well as by the electron donating strength of the DMB ligand located in the trans position (30). The DMB ligand, which is normally a good electron donor, acts as a poor electron donor for alkylcobalamins due to steric repulsions between the DMB ligand and the corrin ring that result in a very long Co—N (axial) distance of 2.20 Å. This long Co—N (DMB) distance has been observed in crystal data for AdoCbl (31) and MeCbl (32) and recently has been confirmed by extended x-ray absorption fine structure (EXAFS) spectroscopy of solution samples (15, 33). However, previous EXAFS results for the reduction of AdoCbl to Co(II) B_{12} indicate a five-coordinate structure where the Co—N bond to the DMB ligand becomes stronger subsequent to Co—C bond homolysis (15) (Table 2). A recent crystal structure of Co(II) B_{12} by Krautler et al. (34) shows the formation of a distorted square pyramidal intermediate but a smaller effect on the Co—DMB distance. The crystal data also indicate that cobalt moves out of the corrin ring plane toward the DMB ligand by 0.13 Å, presumably reducing the DMB/corrin ring strain. At the same time, the Co—N equatorial distances show minimal change from MeCbl and AdoCbl. Both x-ray crystallographic and EXAFS indicate a reduction in the Co—DMB bond distance for the Co(II) B_{12} intermediate. Co(I) B_{12} also shows no change in the Co—N (equatorial) distances when compared with other B_{12} species. This suggests that modulation of the Co—DMB bond, in the absence of other changes in the corrin ring, is a key mechanism in promoting homolytic versus heterolytic cleavage.

Both methionine synthetase (6, 35), which mediates the transfer of a methyl group from N^5-methyltetrahydrofolate to homocystine, and the coronoid/iron-sulfur protein of *Clostridium thermoaceticum* (7, 8), which acts as a methyl carrier in the formation of acetyl-CoA, are recognized as proceeding through a heterolytically generated Co(I) B_{12} intermediate. For methionine synthetase, the active form of the enzyme cycles between a Co(I) form and MeCbl (6, 35). A Co(II) form of methionine synthase, created by occasional oxidation of Co(I)

TABLE 2 Comparison of EXAFS and x-ray crystallographic results for cobalamin compounds

Compound	EXAFS	X ray
	Å	
Co(III) methylcobalamin		
Co—N (eq)	1.90 ± 0.01[33]	1.89[32]
Co—N (ax)	2.20 ± 0.03	2.19
Co—C	2.00 ± 0.03	1.99
Estimated SD		0.02
Co(II) B_{12}		
Co—N (eq)	1.88 ± 0.02[15]	1.89[34]
Co—N (ax)	1.99 ± 0.03	2.13
Estimated SD		0.02
Co(I) B_{12}		
Co—N (eq)	1.88 ± 0.02	—

The Co—N (equatorial) distance for the two x-ray solutions are the $1/r^2$ average of the four individual equatorial distances. EXAFS results for Co(I), Co(II) B_{12}, and methylcobalamin are from solution samples. Bond distance entries correspond to cobalt-nitrogen equatorial (eq), axial (ax), and axial cobalt-carbon coordinations. Estimated SD are noted for structures determined by x-ray crystallography.

during the enzymatic cycle, is inactive (6). The work of Ragsdale et al. (7) and Harder et al. (8) on the coronoid/iron-sulfur protein from *C. thermoaceticum* provide evidence of a base-off MeCbl cycled to a Co(I) B_{12} intermediate in the enzymatic pathway. This result is of particular importance because our EXAFS and x-ray edge studies confirm the four-coordinate nature of the Co(I) intermediate. Studies by Lexa and Saveant (28, 29) demonstrate that the standard reduction potential from Co(II) to Co(I) B_{12} is less negative for the base-off Co(II) form and that strong axial coordination of the DMB ligand makes generation of the Co(I) species more difficult thermodynamically and kinetically. Our previous EXAFS solution for Co(II) B_{12} provides structural evidence for this stronger coordination, relative to the weak bonding exhibited by AdoCbl and MeCbl. It is also well known that the base-off forms of cobalamins are resistant to homolytic thermolysis relative to the base-on species (36). Thus, a base-off configuration for *C. thermoaceticum* both decreases the tendency for homolytic cleavage and increases the tendency for formation of square planar Co(I) B_{12}.

We thank Syed Khalid and Mike Sullivan for technical assistance at beamline X-9A. We also thank Britton Chance for advice and encouragement and Geoffrey B. Jameson for helpful comments and suggestions.

This research is based on work supported in part by the NRICGP-CSRS, U.S. Department of Agriculture, under agreement 91-37200-6180 of the Program in Human Nutrition, by a grant from the Upjohn Company, and a Grant-in-Aid of Research from the National Academy of Sciences, through Sigma Xi, Scientific Research Society (M.D.W.). The construction and operation of beamline X-9A is supported by National Institute of Health grant, RR-01633, and National Science Foundation grant, DMR-85190959. The National Synchrotron Light Source is supported by the Department of Energy, Division of Materials Sciences, and Division of Chemical Sciences.

Received for publication 17 September 1991 and in final form 3 March 1992.

REFERENCES

1. Glusker, J. P. 1982. X-ray crystallography of B_{12} and cobaloximes. *In* B_{12}. Vol. 1. D. Dolphin, editor. John Wiley & Sons, New York. 23–106.
2. Halpern, J. 1985. Mechanisms of coenzyme B_{12}-dependent rearrangements. *Science (Wash. DC).* 227:869–875.
3. Halpern, J. 1982. Determination and significance of transition metal-alkyl bond dissociation energies. *Acc. Chem. Res.* 15:238–244.
4. Hay, B. P., and R. G. Finke. 1986. Thermolysis of the Co—C bond of adenosylcobalamin. 2. Products, kinetics, and Co—C bond dissociation in aqueous solution. *J. Am. Chem. Soc.* 108:4820–4829.
5. Hay, B. P., and R. G. Finke. 1987. Thermolysis of the Co—C bond in adenosylcobalamin. 3. Quantification of the axial base effect in adenosylcobalamin by the synthesis and thermolysis of axial base-free adenosylcobinamide. Insights into the energetics of enzyme-assisted cobalt-carbon bond homolysis. *J. Am. Chem. Soc.* 109:8012–8018.
6. Frasca, V., R. V. Banerjee, W. R. Dunham, R. H. Sands, and R. G. Matthews. 1988. Cobalamin-dependent methionine synthase from *Escherichia coli B:* electron paramagnetic resonance spectra of the inactive form and the active methylated form of the enzyme. *Biochemistry.* 27:8458–8465.
7. Ragsdale, S. W., P. A. Lindahl, and E. Munck. 1987. Mossbauer, EPR, and optical studies of the corrinoid, iron-sulfur protein involved in the synthesis of acetyl coenzyme A by *Clostridium thermoaceticum. J. Biol. Chem.* 262:14289–14297.
8. Harder, S. R., W. P. Lu, B. A. Feinberg, and S. W. Ragsdale. 1989. Spectrochemical studies of the corrinoid/iron-sulfur protein involved in acetyl coenzyme A synthesis by *Clostridium thermoaceticum. Biochemistry.* 28:9080–9087.
9. Dolphin, D. 1970. Preparation of the reduced forms of vitamin B_{12} and of some analogs of the vitamin B_{12} coenzyme containing a cobalt-carbon bond. *Methods Enzymol.* 18C:34–52.
10. Beaven, G. H., and E. A. Johnson. 1955. The reduction of vitamin B_{12}. *Nature (Lond.).* 176:1264–1265.
11. Wirt, M. D., I. Sagi, E. Chen, S. M. Frisbie, R. Lee, and M. R. Chance. 1991. Geometric conformations of intermediates of B_{12} catalysis by x-ray edge spectroscopy: Co(I) B_{12}, Co(II) B_{12}, and base-off adenosylcobalamin. *J. Am. Chem. Soc.* 113:5299–5304.
12. Powers, L. S., B. Chance, Y. Ching, and P. Angiollo. 1981. Structural features and the reaction mechanism of cytochrome oxidase. Iron and copper x-ray absorption fine structure. *Biophys. J.* 34:465–498.
13. Gmur, N. F., W. Thomlinson, and S. White-DePace. 1989. National Synchrotron Light Source User's Manual: Guide to the VUV and X-Ray Beamlines. 3rd ed. BNL 42276 Informal Report. NTIS X9A.
14. Khalid, S. M., G. Rosenbaum, and B. Chance. 1986. Economical efficient detector for fluorescent x-ray absorption spectroscopy. *SPIE.* 690:65–68.
15. Sagi, I., M. D. Wirt, E. Chen, S. M. Frisbie, and M. R. Chance. 1990. Structure of an intermediate of coenzyme B_{12} catalysis by EXAFS: Co(II)B_{12}. *J. Am. Chem. Soc.* 112:8639–8644.
16. Chance, M. R., L. S. Powers, C. Kumar, and B. Chance. 1986. X-ray absorption studies of myoglobin peroxide reveal functional differences between globins and heme enzymes. *Biochemistry.* 25:1259–1265.
17. Lee, P., P. Citrin, P. Eisenberger, and B. Kincaid. 1981. Extended x-ray absorption fine structure—its strengths and limitations as a structural tool. *Rev. Mod. Phys.* 53:769–806.
18. Stevens, E. J. 1981. Electronic structure of metalloproteins. 1. Experimental electron density distribution of (*meso*-tetraphenylporphinato)cobalt(II). *J. Am. Chem. Soc.* 103:5087–5095.
19. Lytle, F. W., D. E. Sayers, and E. A. Stern. 1989. Report of the international workshop on standards and criterion in x-ray absorption spectroscopy. *Physica B.* 158:701–722.
20. Chance, M. R., L. S. Powers, T. Poulos, and B. Chance. 1986. Cytochrome c peroxidase compound ES is identical with horseradish peroxidase compound I in iron-ligand distances. *Biochemistry.* 25:1266–1270.
21. Chance, M. R., L. Parkhurst, L. S. Powers, and B. Chance. 1986. Movement of Fe with respect to the heme plane in the R-T transition of carp hemoglobin. An extended x-ray absorption fine structure study. *J. Biol. Chem.* 261:5689–5692.
22. Bart, C. 1986. Near-edge x-ray absorption spectroscopy in catalysis. *In* Advances in Catalysis. D. D. Eley, H. Pines, and P. B. Weisz, editors. Academic Press, Orlando, FL. 203–296.
23. Roe, A. L., D. J. Schneider, R. J. Mayer, J. W. Pyrz, J. Widom, and

L. Que, Jr. 1984. X-ray absorption spectroscopy of iron-tyrosinate proteins. *J. Am. Chem. Soc.* 106:1676–1681.

24. Blair, R. A., and W. A. Goddard. 1980. Ab *initio* studies of the X-ray absorption edge in copper complexes. I. Atomic Cu^{2+} and $Cu(II)Cl_2$. *Physical Rev. B.* 22:2767–2776.
25. Kosugi, N., T. Yokoyama, K. Asakura, and H. Kuroda. 1984. Polarized Cu k-edge XANES of square-planar $CuCl_4^{2-}$ ion. Experimental and theoretical evidence for shake-down phenomena. *Chem. Phys.* 91:249–256.
26. Kosugi, N., T. Yokoyama, and H. Kuroda. 1986. Polarization dependence of XANES of square-planar $Ni(CN)_4^{2-}$ ion. A comparison with octahedral $Fe(CN)_6^{4-}$ and $Fe(CN)_6^{3-}$ ions. *Chem. Phys.* 104:449–453.
27. Giannotti, C. 1982. Electronic spectra of B_{12} and related systems. *In* B_{12}. Vol. 1. D. Dolphin, editor. John Wiley & Sons, New York. 418–419.
28. Lexa, D., and J. M. Saveant. 1983. The electrochemistry of vitamin B_{12}. *Acc. Chem. Res.* 16:235–243.
29. Lexa, D., and J. M. Saveant. 1976. Electrochemistry of vitamin B_{12}. I. Role of the base-on/base-off reaction in the oxidoreduction mechanism of the B_{12r}-B_{12s} system. *J. Am. Chem. Soc.* 98:2652–2658.
30. Marzilli, L. C., M. F. Summers, N. Bresciani-Pahor, E. Zangrando, J. P. Charland, and L. Randaccio. 1985. Rare examples of structurally characterized five-coordinate organocobalt complexes. Novel dynamic NMR evidence for synergistic enhancement of cis and trans effects in B_{12} models. *J. Am. Chem. Soc.* 107:6880–6888.
31. Savage, H. F., P. F. Lindley, J. L. Finney, and P. A. Timmins. 1987. High resolution neutron and x-ray refinement of vitamin B_{12} coenzyme, $C_{72}H_{100}CoN_{18}O_{17}P \cdot 17H_2O$. *Acta Cryst.* 43B: 280–296.
32. Rossi, M., J. P. Glusker, L. Randaccio, M. F. Summers, P. J. Toscano, and L. G. Marzilli. 1985. The structure of a B_{12} coenzyme: methylcobalamin studies by x-ray and NMR methods. *J. Am. Chem. Soc.* 107:1729–1738.
33. Sagi, I., and M. R. Chance. 1991. EXAFS analysis of vitamin B_{12} and related cobalamins. *Biophys. J.* 59:365A. (Abstr.)
34. Krautler, B., W. Keller, and C. Kratky. 1989. Coenzyme B_{12} chemistry: the crystal and molecular structure of cob(II)alamin. *J. Am. Chem. Soc.* 111:8936–8938.
35. Banerjee, R. V., and R. G. Matthews. 1990. Cobalamin-dependent methionine synthase. *FASEB* (*Fed. Am. Soc. Exp. Biol.*) *J.* 4:1450–1459.
36. Chemaly, S. M., and J. M. Pratt. 1980. The chemistry of vitamin B_{12}. Part 19. Labilisation of the cobalt-carbon bond on organocobalamins by steric distortions; neopentyl-cobalamin as a model for labilisation of the vitamin B_{12} coenzymes. *J. Chem. Soc. Dalton Trans.* 2274–2281.